High Speed VCSELs and VCSEL Arrays for Single and Multicore Fiber Interconnects

Anders Larsson*, Petter Westbergh, Johan S. Gustavsson, Erik Haglund and Emanuel P. Haglund
Photonics Laboratory, Department of Microtechnology and Nanoscience,
Chalmers University of Technology, SE-41296, Göteborg, Sweden

ABSTRACT

Our recent work on high speed 850 nm VCSELs and VCSEL arrays is reviewed. With a modulation bandwidth approaching 30 GHz, our VCSELs have enabled transmitters and links operating at data rates in excess of 70 Gbps (at IBM) and transmission over onboard polymer waveguides at 40 Gbps (at University of Cambridge). VCSELs with an integrated mode filter for single mode emission have enabled transmission at 25 Gbps over > 1 km of multimode fiber and a speed-distance product of 40 Gbps·km. Dense VCSEL arrays for multicore fiber interconnects have demonstrated 240 Gbps aggregate capacity with excellent uniformity and low crosstalk between the 40 Gbps channels.

Keywords: optical interconnect, vertical cavity surface emitting laser, high speed modulation, multicore fiber

1. INTRODUCTION

Optical interconnects (OIs) are being deployed at large scale in datacenters, supercomputers and data storage systems to meet requirements of higher interconnect capacity, bandwidth density and energy efficiency [1,2]. VCSEL-based OIs, using multimode fibers (MMF) or polymer waveguides as the transmission medium, are attractive as they enable the cost and power efficiency needed for short reach inter- and intra-rack [3] and onboard interconnectivity [4].

To reach an aggregate OI capacity in the multi-Tbps range and a higher bandwidth density, lane rates are expected to increase from today's 25-28 Gbps to 100 Gbps (e.g. for 1.6 Tbps Ethernet) [5]. At the same time, the interconnect energy consumption (energy consumed in driver IC + VCSEL + photodiode + receiver IC) has to be reduced from today's 10's of pJ/bit to the 1 pJ/bit level, also at the very high lane rates [6]. Additionally, the OI transceivers have to be able to operate at a high ambient temperature (85°C, at least) over an extended period of time. Finally, while most of today's VCSEL-based interconnect cables span distances from 1 to 300 m there is a need for both longer and shorter interconnect distances as e.g. datacenters grow in size [1] and OIs migrate closer to the onboard ASICs (embedded optics) [2].

A significant increase of the lane rate of VCSEL-based OIs is possible with the development of higher speed optoelectronics (VCSELs and photodiodes) and electronics (transmitter and receiver ICs) and the use of electronic compensation techniques (e.g. pre-distortion, equalization, forward error correction) [7] and higher order modulation formats (e.g. PAM, DMT) [8,9]. This will enable 100 Gbps transmission over a single fiber with a single core on a single wavelength. The use of multiple (parallel) fibers will bring the aggregate OI capacity to the 1 Tbps level. A further increase to the 10 Tbps level is enabled by more aggressive use of spatial division multiplexing (SDM) or wavelength division multiplexing (WDM): multiple fibers with multiple cores and a single wavelength [10] or multiple fibers with a single core and multiple wavelengths [11]. Combining these techniques (multiple fibers with multiple cores and multiple wavelengths) will finally bring the aggregate OI capacity to the 100 Tbps level. This is all illustrated in Fig.1. Such a scenario calls for the development of higher speed and more energy efficient VCSELs, dense arrays of high speed VCSELs for multicore fibers (MCFs) and multi-wavelength arrays of high speed VCSELs.

Here we present an overview of recent work at Chalmers University of Technology to develop high speed VCSELs and VCSEL arrays for single- and multicore fiber interconnects. The VCSELs are all GaAs-based, oxide confined VCSELs and emit at 850 nm, the standard wavelength in existing datacom and computercom standards.

*anders.larsson@chalmers.se; phone +46-703-088626; fax +46-31-7721540; www.chalmers.se

Vertical-Cavity Surface-Emitting Lasers XIX, edited by Chun Lei, Kent D. Choquette, Proc. of SPIE
Vol. 9381, 93810D · © 2015 SPIE · CCC code: 0277-786X/15/$18 · doi: 10.1117/12.2082614

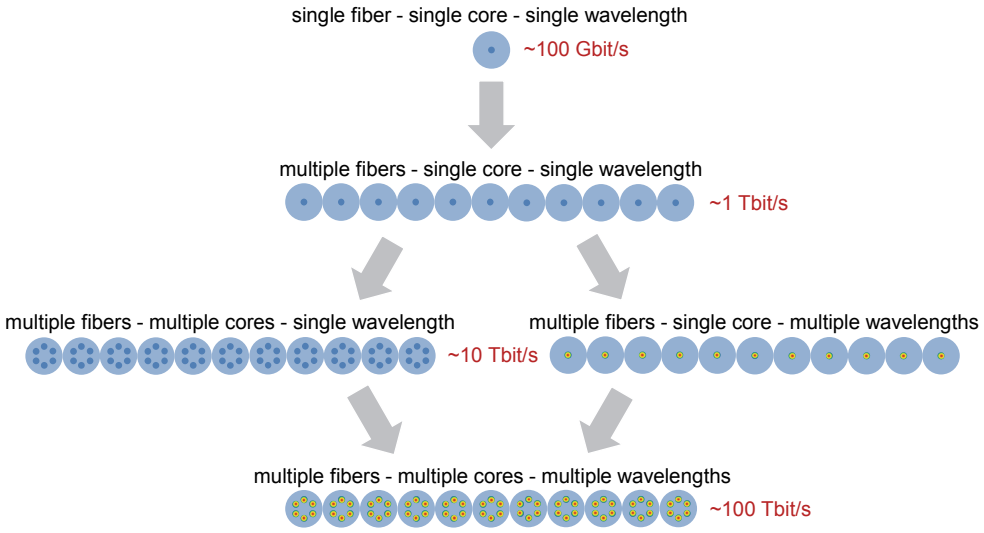

Figure 1. Evolution of VCSEL-based OIs towards 100 Tbps aggregate capacity through higher speed optoelectronics and electronics and the use of electronic compensation techniques, higher order modulation formats and SDM/WDM.

2. HIGH SPEED VCSELs FOR SINGLE CORE FIBER INTERCONNECTS

2.1 High speed VCSEL design

The modulation speed of a VCSEL is limited by the damping of the resonant electron-photon interaction and by effects of self-heating and electrical parasitics [12]. Guidelines for the design of high speed VCSELs can be derived from a simple single mode rate equation analysis, which yields the following expressions for the resonance frequency (f_r) and the damping rate (γ) of the intrinsic small signal modulation response [13]:

$$f_r = D \cdot \sqrt{I - I_{th}} \quad ; \quad D = \frac{1}{2\pi}\sqrt{\frac{\eta_i \Gamma v_g}{qV_a}\frac{\partial g/\partial n}{\chi}} \tag{1}$$

$$\gamma = K \cdot f_r^2 + \gamma_0 \quad ; \quad K = 4\pi^2\left(\tau_p + \frac{\varepsilon \cdot \chi}{v_g \cdot \partial g/\partial n}\right) \tag{2}$$

A large modulation bandwidth is favored by a large *D*-factor which enables a rapid increase of the resonance frequency with current (I). This calls for a VCSEL design with a high internal quantum efficiency (η_i), large optical confinement factor (Γ), high differential gain in the quantum wells ($\partial g/\partial n$), small active region volume (V_a) and efficient transport and capture of carriers in the active region (χ). Also, for large bandwidth, the damping of the modulation response, quantified by the *K*-factor, cannot be too high. This again calls for high differential gain and efficient transport and capture of carriers, as well as small gain compression (ε) and a short cavity photon lifetime (τ_p). Note, however, that these fundamental VCSEL parameters cannot be independently optimized which calls for tradeoffs in the design.

With the modulation speed of VCSELs being largely limited by parasitics and thermal effects it is also of utmost importance to reduce the VCSEL resistance and capacitance (which largely stems from charge stored over the oxide layers) and to minimize heat generation (Joule heating and internal optical loss) and thermal impedance.

Our first generation (Gen1) VCSELs [14] employed strained InGaAs/AlGaAs quantum wells (QWs) for high differential gain [15], a graded composition confinement structure for fast transport and capture of carriers in the QWs, a $3\lambda/2$ optical cavity, rather simple interface grading and modulation doping schemes in the distributed Bragg reflectors (DBRs) for low resistance and low internal optical loss, a double oxide aperture for low capacitance and a binary low index compound (AlAs) in most of the bottom DBR for low thermal impedance. This resulted in a modulation bandwidth of 20 GHz [16] which enabled transmission up to 32 Gbps [17].

With the speed of the Gen1 VCSELs largely limited by capacitance [18], we introduced an additional four (secondary) oxide apertures, with an aperture diameter larger than that of the two primary oxide apertures used to confine the current and the optical fields, in the second generation (Gen2) to further reduce the oxide capacitance [19]. Additionally, after realizing the large impact of damping on the modulation response and the bandwidth we used fine-tuning of the photon lifetime to maximize speed [20]. This enabled a 23 GHz modulation bandwidth [21] and transmission up to 40 Gbps [22].

In our third generation (Gen3) VCSELs [23], we reduced the length of the optical cavity to λ/2 to increase the optical confinement factor and reduce the carrier transport and capture times, which led to the use of abrupt interfaces in the carrier confinement structure. Additionally, we used more advanced interface grading and modulation doping schemes in the DBRs for further reductions of resistance and optical loss. The Gen3 design is shown in Fig.2. The performance of the Gen3 VCSELs is presented in sections 2.2 and 2.3.

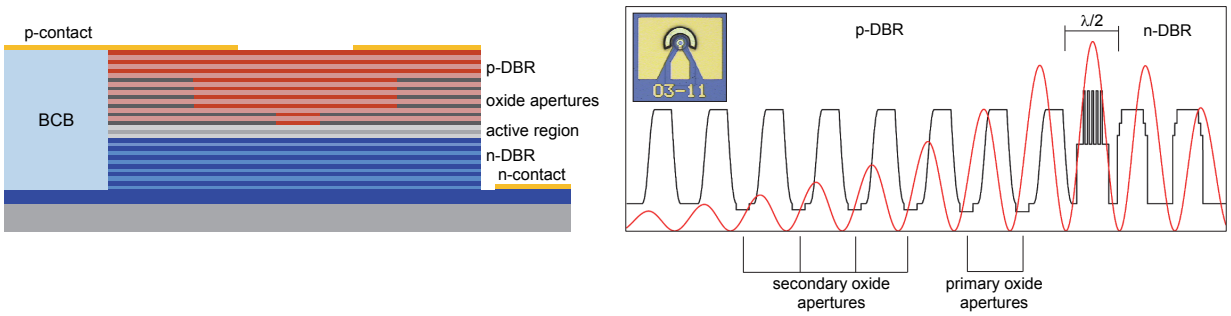

Figure 2. Left: Cross-section of the Gen3 VCSEL showing the multiple oxide apertures. Right: Longitudinal variations of the refractive index and the optical field intensity, with inset showing a microscope image of the VCSEL chip.

Fine-tuning of the photon lifetime is achieved by precise, post-growth thinning of the top layer of the top DBR by dry etching. With the thickness of the top layer being λ/4, the phase of the reflection at the surface is in-phase with the reflections at the DBR interfaces and the top DBR reflectivity is high, yielding photon lifetimes of 4-6 ps (depending on DBR design). With the entire top layer removed, there is an anti-phase reflection at the surface and the top DBR reflectivity is reduced, yielding photon lifetimes of 0.5-1 ps. Thus, large variations of photon lifetime, and therefore damping, is achieved by precise thinning of the top layer.

All VCSELs employ a thick layer of BCB under the p-bond pad to reduce the pad capacitance.

2.2 Basic performance and impact of photon lifetime

Representative performance characteristics of the Gen3 VCSELs are shown in Fig.3 and 4 [24]. Fig.3 shows light-current-voltage characteristics for 4 and 7 μm primary oxide aperture VCSELs. The VCSELs are characterized by high output power, high slope efficiency (0.75 W/A) and differential resistances of 160 and 80 Ω, respectively.

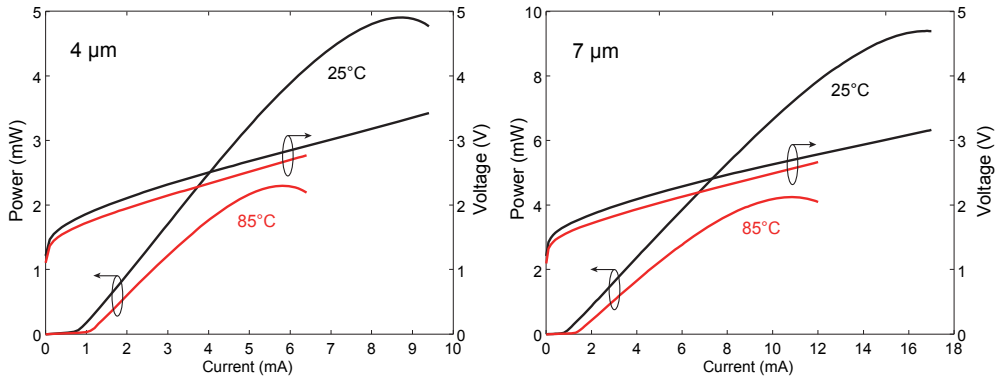

Figure 3. Output power and voltage vs. current at 25 and 85°C for Gen3 VCSELs with primary oxide aperture diameters of 4 μm (left) and 7 μm (right).

Fig.4 shows the small signal modulation response of the Gen3 VCSELs in Fig.3 [24]. The smaller aperture VCSEL reaches a record modulation bandwidth of 28 GHz while the larger aperture VCSEL has a maximum modulation bandwidth of 26 GHz. At a higher temperature of 85°C, the bandwidth still exceeds 20 GHz for both VCSELs.

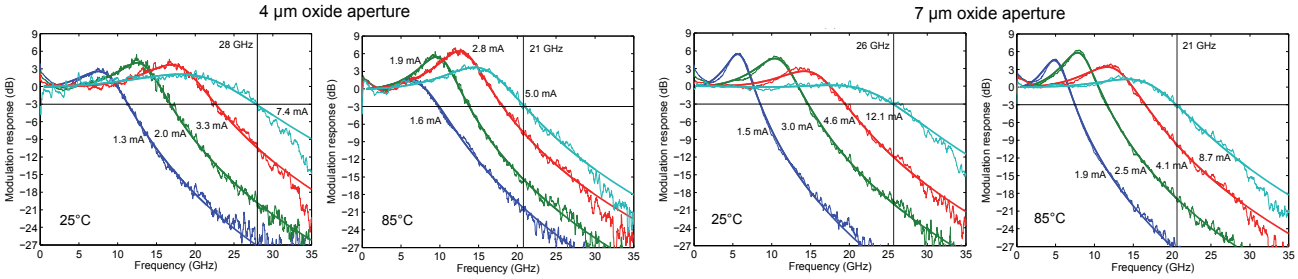

Figure 4. Small signal modulation response at different bias currents and at 25 and 85°C for Gen3 VCSELs with primary oxide aperture diameters of 4 µm (left) and 7 µm (right).

The photon lifetime has large impact on both static and dynamic VCSEL characteristics. Fig.5 shows the results from a study of the dependence of the light-current characteristics and the small signal modulation response on photon lifetime for a series of Gen2 VCSELs with photon lifetimes from 1.2 to 6.4 ps and corresponding *K*-factors from 0.14 to 0.35 ns [20]. The increase of slope efficiency with reduced photon lifetime is beneficial for large signal modulation as the optical modulation amplitude is increased at a given modulation current. The modulation response reveals a rapid increase of the modulation bandwidth from 15 to 23 GHz as the photon lifetime is reduced from 6.4 to 3.3 ps. A further reduction of photon lifetime results in a reduction of the bandwidth. This is a result of a tradeoff between resonance frequency and damping rate.

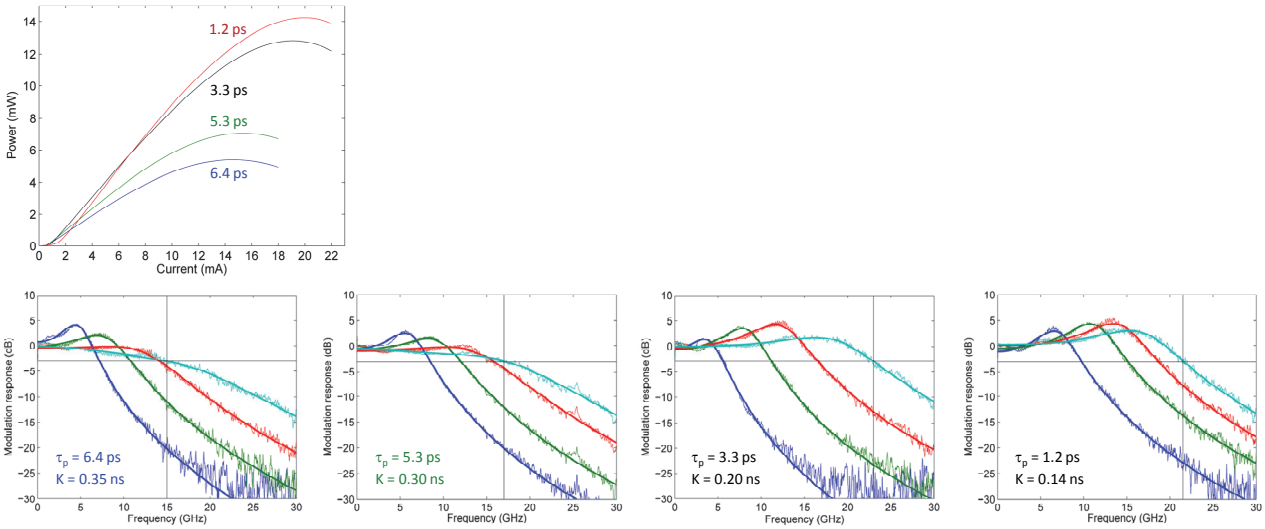

Figure 5. Output power vs. current (upper) and small signal modulation response at different bias currents (lower) for Gen2 VCSELs with different photon lifetimes.

While there is a certain, design dependent photon lifetime that maximizes the modulation bandwidth, it is not clear whether this photon lifetime is the optimum for large signal modulation and data transmission as a less damped VCSEL not only exhibits faster rise and fall times but also stronger relaxation oscillations. The dependence of large signal NRZ modulation on damping is illustrated in Fig.6 for another set of Gen2 VCSELs with *K*-factors from 0.1 to 0.4 ns [25]. Large damping (K = 0.4 ns) results in vertical eye closure due to lower slope efficiency and increased intersymbol interference due to slower rise and fall times while small damping (K = 0.1 ns) results in horizontal eye closure due to excessive data dependent timing jitter caused by the relaxation oscillations. The optimum damping, and thus the optimum photon lifetime, therefore depends on the bit rate, with more damping affordable at low bit rates and less

damping needed at high bit rates. This was confirmed by measurements of the receiver sensitivity required for error-free transmission at different bit rates for VCSELs with different *K*-factors [25].

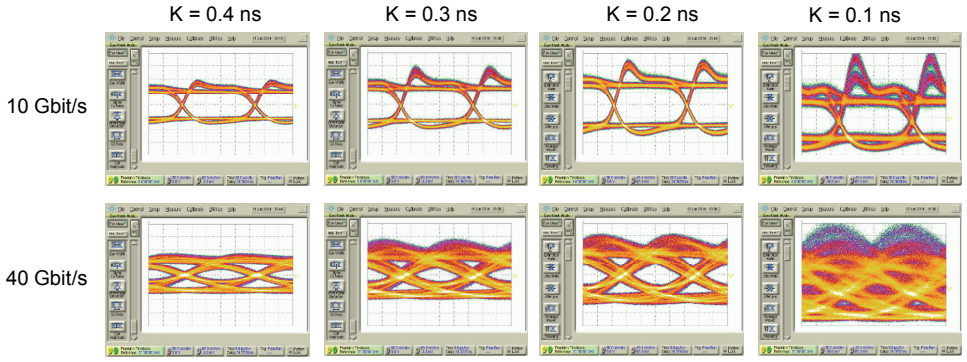

Figure 6. Eye diagrams recorded at 10 and 40 Gbps for Gen2 VCSELs with *K*-factors from 0.1 to 0.4 ns.

2.3 Data transmission

With the VCSEL bandwidth approaching 30 GHz, optical link performance is to a large extent also limited by the performance of the optical receiver and the electronics used to drive the VCSEL and receive the signal from the photodiode. The dependence on optical receiver performance and design is illustrated by the transmission experiments in Fig.7 and 8 where 7-8 µm aperture Gen3 VCSELs were used. In Fig.7, a limiting optical receiver with a bandwidth of 30 GHz is used to achieve error-free transmission at 40 Gbps up to 85°C and at 47 Gbps at 25°C [26]. In Fig.8, a linear optical receiver with a bandwidth of only 22 GHz is used to achieve transmission up to 57 Gbps at 25°C [27].

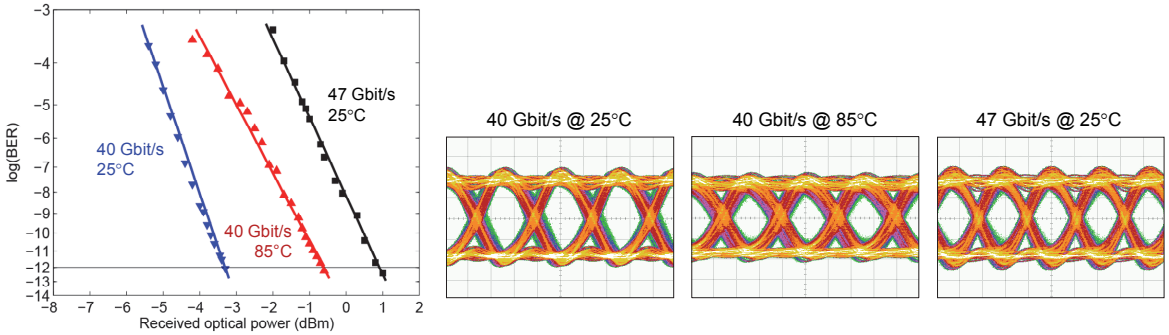

Figure 7. Results from high bit rate MMF transmission using a 30 GHz limiting optical receiver. Left: BER vs. received optical power at 40 and 47 Gbps. Right: Corresponding received eyes at BER = 10^{-12}.

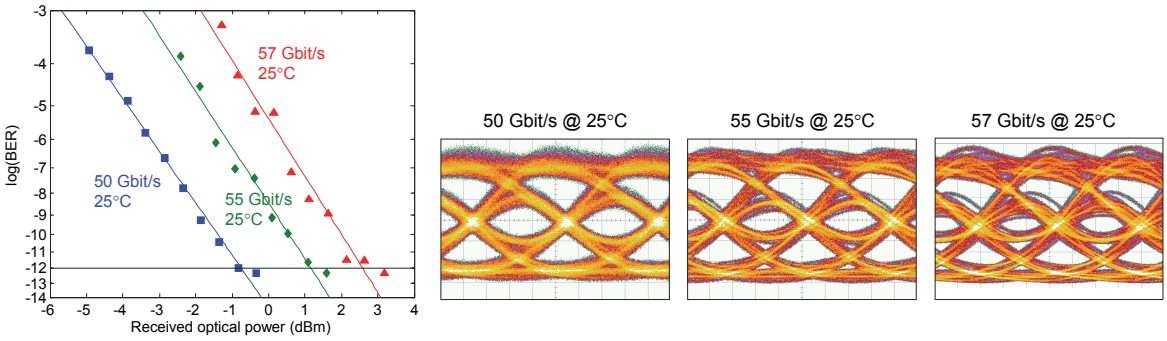

Figure 8. Results from high bit rate MMF transmission using a 22 GHz linear optical receiver. Left: BER vs. received optical power at 50, 55 and 57 Gbps. Right: Corresponding received eyes at BER = 10^{-12}.

A significant increase of the lane rate can also be achieved through the use of driver and receiver electronics designed to mitigate bandwidth limitations imposed by the optoelectronics (VCSEL and photodiode) and the optical fiber [7]. Recent work at IBM, using a 5 µm aperture Gen3 VCSEL, a 30+ GHz photodiode and 130 nm SiGe BiCMOS drivers and receiver amplifiers with two-tap linear feed forward equalization, has demonstrated error-free transmission over 7 m of MMF fiber at bit rates up 71 Gbps [28]. This is the highest bit rate of any optical link using a directly NRZ modulated semiconductor laser. IBM also demonstrated transmission at bit rates up to 50 Gbps with the transmitter held at a temperature of 90°C [29].

Polymer waveguides are promising for use in board-level interconnections as they can be directly integrated onto printed circuit boards [4]. Recent work at University of Cambridge, using a 9 µm aperture Gen3 VCSEL, has demonstrated error-free transmission over a 1 m long multimode polymer waveguide at a bit rate of 40 Gbps [30]. This represents a record speed-distance product of 40 Gbps·m for an onboard optical interconnect and is enabled by the high optical power and high slope efficiency of the high speed VCSEL as the power budget, rather than the link bandwidth, limits performance due to the relatively large waveguide loss (0.04 dB/cm) and the long, backplane compatible waveguide.

2.4 High speed VCSELs for extended reach

The transmission distance for an optical link with a multimode VCSEL and a high modal bandwidth MMF (e.g. OM4) is limited by chromatic dispersion in the optical fiber. Therefore, extended reach can be achieved by reducing the spectral width of the VCSEL, i.e. using single or quasi-single mode VCSELs [31].

By reducing the diameter of the primary oxide apertures of a Gen2 VCSEL to 3 µm, we have previously demonstrated transmission over 1100 m of MMF at 20 Gbps and over 500 m at 25 Gbps [32]. This VCSEL is quasi-single mode with a spectral rms width of 0.3 nm. However, the small oxide aperture leads to high current density and high differential resistance, and therefore a high internal temperature, which may compromise the long term reliability. We have therefore developed a new design where single mode emission is achieved with a larger oxide aperture (6 µm) by the integration of a 3 µm diameter transverse mode filter (Fig.9) [33]. The mode selective loss provided by the mode filter results in >30 dB suppression of higher order modes and a spectral rms width of 0.25 nm. This VCSEL has enabled transmission over 1300 m of MMF at 25 Gbps and over 2000 m at 20 Gbps. The latter represents a record speed-distance product for VCSEL-MMF links of 40 Gbps·km [34].

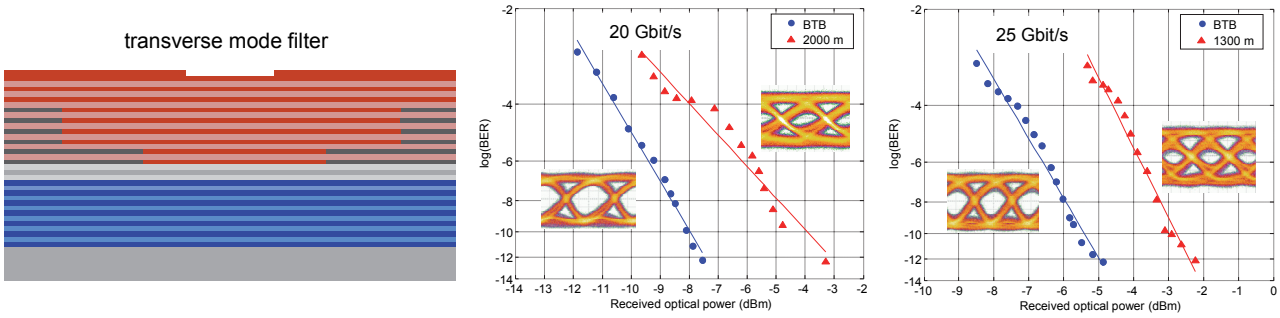

Figure 9. Left: High speed VCSEL with an integrated transverse mode filter for single mode emission. Middle and right: BER vs. received optical power at 20 and 25 Gbps at different MMF transmission distances. The insets show the received eyes.

3. HIGH SPEED VCSEL ARRAYS FOR MULTICORE FIBER INTERCONNECTS

A promising solution for higher aggregate OI capacity and bandwidth density is the use of MCFs [10]. For this purpose we have designed and fabricated dense 6-channel VCSEL arrays, matching the outer six cores of a seven-core MCF with 26 µm diameter graded index multimode cores and a 39 µm core-to-core spacing [10]. Our VCSEL array design aims at a channel speed of 40 Gbps for an aggregate capacity of 240 Gbps with sufficiently low levels of inter-channel RF, optical and thermal crosstalk.

3.1 VCSEL array design and fabrication

Microscope images of the VCSEL array are shown in Fig.10. The six VCSELs are uniformly distributed on a circle with a radius of 39 µm, yielding a VCSEL center-to-center distance of 39 µm to match the outer cores of the MCF. The Gen3 epitaxial VCSEL material was used for array fabrication. Fabrication starts with etching of top mesas and selective oxidation to form 8 µm diameter apertures in the primary oxide layers of each VCSEL. A common cathode is created by etching a large bottom mesa to the n-contact layer. The array is planarized with BCB and contacts, transmission lines and bond pads are finally deposited. Each VCSEL in the array has a ground-signal-ground contact for high frequency probing.

As a post-fabrication step, the top layer of the top DBR was thinned to adjust the photon lifetime [20], and therefore the damping, for a flat and high bandwidth modulation response suitable for high speed data transmission.

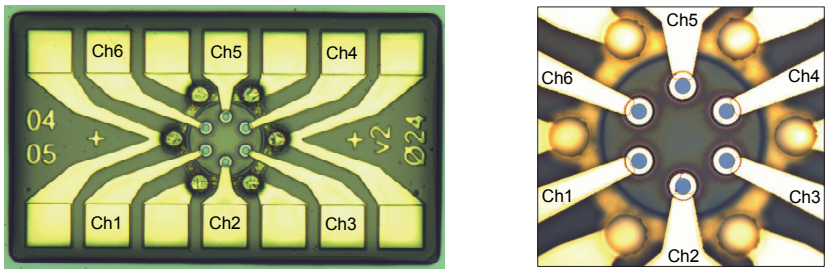

Figure 10. Left: Microscope image of the 6-channel VCSEL array (chip size: 720 x 420 µm^2). Right: Close-up of the central region of the array showing the six VCSELs and the common bottom mesa (cathode) configuration.

3.2 Performance and array uniformity

Fig.11 shows the light-current-voltage characteristics for the individual VCSELs in the array and the variations of threshold current and differential resistance (at 6 mA, the bias current used for data transmission) among the VCSELs [35]. The performance is uniform over the array with high slope efficiency (0.7 W/A at 25°C) and a power variation <0.5 dB over the entire current range, regardless of temperature.

Thermal crosstalk was measured by monitoring the temperature of an individual VCSEL (through spectral measurements) while increasing the current of all other VCSELs to 6 mA. The increase of temperature was less than 5°C and, therefore, the thermal crosstalk is relatively small.

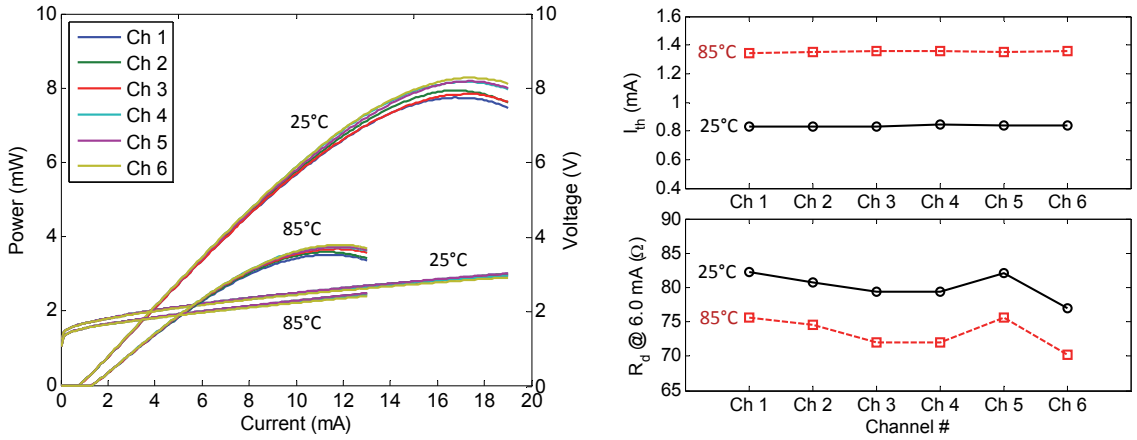

Figure 11. Left: Output power and voltage vs. current at 25 and 85°C for all six VCSELs in the array. Right: Uniformity of threshold current (upper) and differential resistance (lower) over the array.

Fig.12 shows the small signal modulation response at 25°C for the channel 1 VCSEL at different bias currents [35]. The maximum 3 dB bandwidth for all VCSELs at 25 and 85°C is shown in the inset. Again, the performance is uniform across the array with a bandwidth >21 GHz at 25°C and >19 GHz at 85°C.

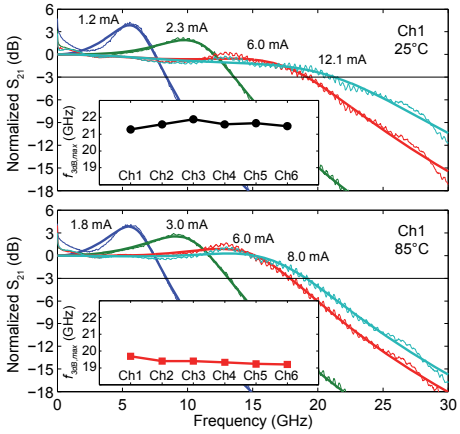

Figure 12. Small signal modulation response at different bias currents for the channel 1 VCSEL at 25°C (upper) and 85°C (lower). The insets shows the uniformity of the maximum modulation bandwidth over the array.

The frequency dependent RF crosstalk between pairs of VCSELs in the array was investigated using S-parameter measurements. The crosstalk was found to be largest between nearest neighbor VCSELs and was measured to be < -35 dB at 20 GHz and < -33 dB at 40 GHz. This level of crosstalk should have no impact on the signal quality.

The performance of individual channels and the uniformity over the array under large signal modulation were investigated using a standard single core MMF (50 µm core) to connect the VCSELs one by one to a 22 GHz linear optical receiver [35]. Measurements were conducted at 25 and 40 Gbps and 25 and 85°C. The bias currents were 6 mA, except at 40 Gbps and 85°C where they were set to 8 mA. Fig.13 shows eye diagrams of the received signal captured at both bit rates and temperatures. Open eyes and excellent uniformity over the arrays are observed under all conditions. Fig.13 also shows the measured bit-error-rate (BER) vs. optical modulation amplitude (OMA) for all channels at both data rates and temperatures. The performance is again uniform among the channels with an OMA penalty of 0.5 dB and 2-3 dB when increasing the temperature from 25 to 85°C at 25 and 40 Gbps, respectively.

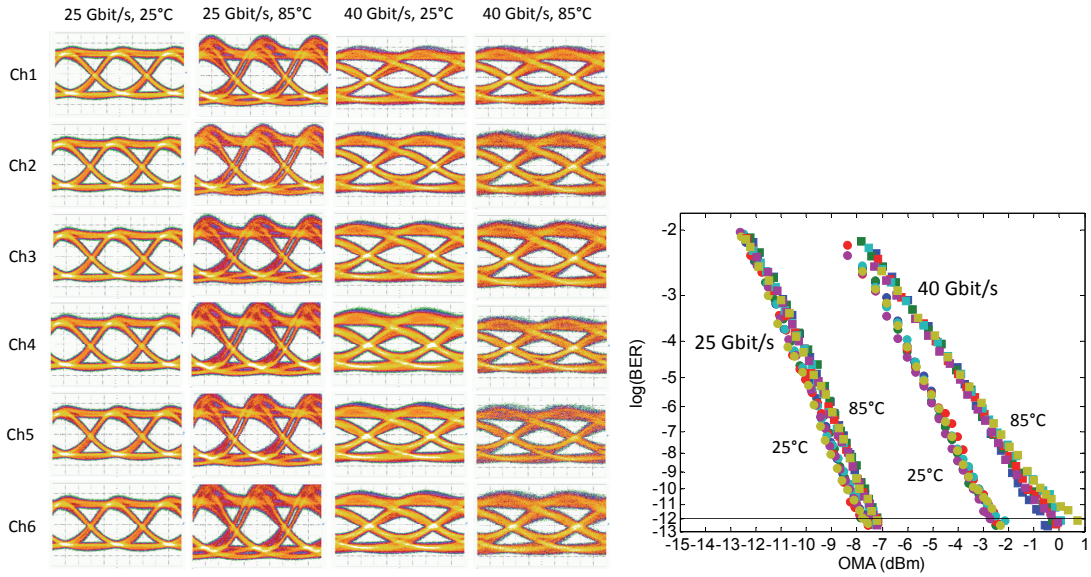

Figure 13. Data transmission on individual channels using a standard SCF. Left: Received eyes at BER = 10^{-12} for all six channels at 25 and 40 Gbps and 25 and 85°C. Right: Corresponding measurements of BER vs. OMA for all channels.

3.3 Multicore fiber transmission and crosstalk

Optical crosstalk was studied by butt-coupling and aligning a MCF to the VCSEL array. With one of the VCSELs biased at 6 mA, the optical power was measured in the other cores of the MCF. The crosstalk was found to be < -20 dB, which is also not expected to have an impact on the signal quality.

Transmission experiments were also conducted with the MCF butt-coupled and aligned to the VCSEL array to study the effects of crosstalk between channels. While transmitting data on one of the channels, asynchronous data was simultaneously transmitted on the two nearest neighbor channels (aggressors). Fig.14 shows the measured BER vs. OMA at bit rates of 25 and 40 Gbps, with and without aggressors. No crosstalk penalty is observed, as expected from the low levels of measured optical and RF crosstalk.

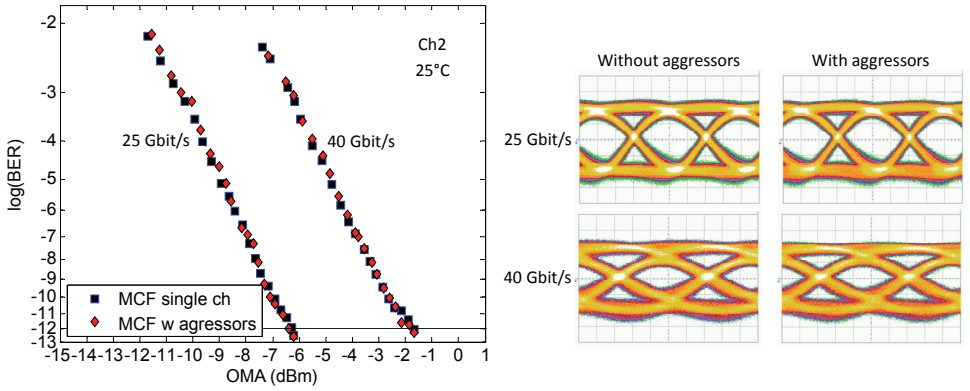

Figure 14. Data transmission over the MCF. Left: BER vs. OMA for channel 2 at 25°C at 25 and 40 Gbps with (red) and without (blue) aggressors on the neighboring channels 1 and 3. Right: Corresponding received eyes at BER = 10^{-12}.

4. SUMMARY

Oxide confined 850 nm VCSELs operating at high speed have been realized using optimized active region and cavity designs, as well as techniques for reducing capacitance and thermal impedance. Investigations of the impact of damping on the small and large signal VCSEL dynamics show that damping has a major impact on the modulation response. While a reduction of damping allows for a small signal modulation bandwidth approaching 30 GHz, it is found that the optimum damping under large signal modulation and data transmission is bit rate dependent. Transmission at data rates up to 47 and 57 Gbps was achieved with limiting and linear optical receivers, respectively. Our VCSELs have also enabled the assembly of equalized transmitters and links operating at 71 Gbps (at IBM) and transmission over onboard polymer waveguides at 40 Gbps (at University of Cambridge).

To enable transmission over long distances of MMF we use an integrated mode filter for single mode emission, thereby mitigating the effects of chromatic dispersion in the fiber. Such VCSELs have enabled transmission at 25 Gbps over 1300 m of MMF and at 20 Gbps over 2000 m. The latter represents a record bandwidth-distance product of 40 Gbps·km.

To enable high bandwidth density interconnects using MCFs, we have developed dense 6-channel VCSEL arrays with each VCSEL operating up to a bit rate of 40 Gbps. The arrays have an aggregate capacity of 240 Gbps and show excellent uniformity. An investigation of RF, optical and thermal crosstalk between the channels revealed very low levels of crosstalk.

ACKNOWLEDGMENT

We would like to thank IQE Europe (A. Joel) for providing the epitaxial VCSEL material, our collaborators at IBM (D. Kuchta) and University of Cambridge (N. Bamiedakis) for their work on transmitter integration and polymer waveguide interconnects, respectively, and OFS (L. Grüner-Nielsen) for providing the MCF. Financial support was received from the Swedish Foundation for Strategic Research and from the European Union's Seventh Framework Program for research, technological development and demonstration under grant agreement no. 607274 (project MERLIN).

REFERENCES

[1] C. DeCusatis, "Optical interconnect networks for data communications", IEEE J. of Lightwave Technol. 32, 544-552 (2014).

[2] M.A. Taubenblatt, "Optical interconnects for high performance computing", IEEE J. of Lightwave Technol. 30, 448-458 (2012).

[3] R.E. Freund, C.A. Bunge, N.N. Ledentsov, D. Molin and C. Caspar, "High speed transmission in multimode fibers", IEEE J. of Lightwave Technol. 28, 569-586 (2010).

[4] K. Schmidtke, F. Flens, A. Worrall, R. Pitwon, F. Betschon, T. Lamprecht and R. Krähenbühl, "960 Gb/s optical backplane ecosystem using embedded polymer waveguides and demonstration in a 12G SAS storage array", IEEE J. Lightwave Technol. 31, 3970-3975 (2013).

[5] C. Cole, "Beyond 100G client interfaces", IEEE Comm. Mag., S58-S66 (2012).

[6] D.A.B. Miller, "Device requirements for optical interconnects to silicon chips", Proc. IEEE 97, 1166-1185 (2009).

[7] D.M. Kuchta, A.V. Rylyakov, C.L. Schow, J.E. Proesel, C. Baks, P. Westbergh, J.S. Gustavsson and A. Larsson, "64 Gb/s transmission over 57 m MMF using an NRZ modulated 850 nm VCSEL", Proc. Optical Fiber Communications Conference, paper Th3C.2 (2014).

[8] C. Cole, I. Lyubomirsky, A. Ghisai and V. Telang, "High order modulation for client optics", IEEE Comm. Mag., 50-57 (2013).

[9] K. Szczerba, P. Westbergh, M. Karlsson, P.A. Andrekson and A. Larsson, "60 Gbit/s error-free 4-PAM operation with 850 nm VCSEL", Electron. Lett. 49, 953-955 (2013).

[10] B.G. Lee, D.M. Kuchta, F.E. Doany, C.L. Schow, P. Pepeljugoski, C. Baks, T.F. Taunay, B. Zhu, M.F. Yan, G.E. Oulundsen, D.S. Vaidya, W. Luo and N. Li, "End-to-end multicore multimode fiber optic link operating up to 120 Gb/s", IEEE J. Lightwave Technol. 30, 886-891 (2012).

[11] B.E. Lemoff, M.E. Ali, G. Panotopoulos, E. De Groot, G.M. Flower, G.H. Rankin, A.J. Schmit, K.D. Djordjev, M.R.T. Tan, A. Tandon, W. Gong, R.P. Tella, B. Law and D.W. Dolfi, "500 Gbps parallel-WDM optical interconnect", Proc. IEEE Electronic Components and Technology Conference, 1027-1031 (2005).

[12] A. Larsson, "Advances in VCSELs for communication and sensing", IEEE Sel. Top. Quantum Electron. 17, 1552-1567 (2011).

[13] L.A. Coldren and S.W. Corzine, *Diode Lasers and Photonic Integrated Circuits*, Wiley, Hoboken, NJ, ch.5.3 (2012).

[14] P. Westbergh, J.S. Gustavsson, Å. Haglund, M. Sköld, A. Joel and A. Larsson, "High speed, low current density 850 nm VCSELs", IEEE J. Sel. Top. Quantum Electron. 15, 694-703 (2009).

[15] S.B. Healy, E.P. O´Reilly, J.S. Gustavsson, P. Westbergh, Å. Haglund, A. Larsson and A. Joel, "Active region design for high speed 850 nm VCSELs", IEEE J. Quantum Electron. 46, 506-512 (2010).

[16] P. Westbergh, J.S. Gustavsson, Å. Haglund, H. Sunnerud and A. Larsson, "Large aperture 850 nm VCSELs operating at bit rates up to 25 Gbit/s", Electron. Lett. 44, 907-908 (2008).

[17] P. Westbergh, J.S. Gustavsson, Å. Haglund, A. Larsson, F. Hopfer, D. Bimberg and A. Joel, "32 Gbit/s multimode fibre transmission using a high speed, low current density 850 nm VCSEL", Electron. Lett. 45, 366-368 (2009).

[18] Y. Ou, J.S. Gustavsson, P. Westbergh, Å. Haglund, A. Larsson and A. Joel, "Impedance characteristics and parasitic speed limitations of high speed 850 nm VCSELs", IEEE Photon. Techn. Lett. 21, 1840-1842 (2009).

[19] M. Azuchi, N. Jikutani, M. Arai, T. Kondo and F. Koyama, "Multioxide layer VCSELs with improved modulation bandwidth", Proc. Conference on Lasers and Electro-Optics/Pacific Rim, 163 (2003).

[20] P. Westbergh, J.S. Gustavsson, B. Kögel, Å. Haglund and A. Larsson, "Impact of photon lifetime on high speed VCSEL performance", IEEE J. Sel. Top. Quantum Electron. 17, 1603-1613 (2011).

[21] P. Westbergh, J.S. Gustavsson, B. Kögel, Å. Haglund, A. Larsson and A. Joel, "Speed enhancement of VCSELs using photon lifetime reduction", Electron. Lett. 13, 938-940 (2010).

[22] P. Westbergh, J.S. Gustavsson, B. Kögel, Å. Haglund, A. Larsson, A. Mutig, A. Nadtochiy, D. Bimberg and A. Joel, "40 Gbit/s error-free operation of oxide confined 850 nm VCSEL", Electron. Lett. 14, 1014-1016 (2010).

[23] P. Westbergh, R, Safaisini, E, Haglund, B. Kögel, J.S. Gustavsson, A. Larsson, M. Geen, R. Lawrence and A. Joel, "High speed 850 nm VCSELs with 28 GHz modulation bandwidth operating error free up to 44 Gbit/s", Electron. Lett. 48, 1145-1147 (2012).

[24] P. Westbergh, R. Safaisini, E. Haglund, J.S. Gustavsson and A. Larsson, “High speed 850 nm VCSELs with 28 GHz modulation bandwidth for short reach communication”, Proc. SPIE 8639, 86390X1-6 (2013).
[25] E.P. Haglund, P. Westbergh, J.S. Gustavsson and A. Larsson, “Impact of damping on high speed large signal VCSEL dynamics”, IEEE J. Lightwave Technol., accepted for publication (2014).
[26] P. Westbergh, R. Safaisini, E. Haglund, J.S. Gustavsson, A. Larsson, M. Geen, R. Lawrence and A. Joel, “High speed oxide confined 850 nm VCSELs operating error-free at 40 Gbit/s up to 85ºC”, IEEE Photon. Techn. Lett. 25, 768-771 (2013).
[27] P. Westbergh, E. P. Haglund, E. Haglund, R. Safaisini, J. S. Gustavsson and A. Larsson, “High-speed 850 nm VCSELs operating error-free up to 57 Gbit/s”, Electron. Lett. 49, 1021-1023 (2013).
[28] D.M. Kuchta, A.V. Rylyakov, F.E. Doany, C.L. Schow, J.E. Proesel, C. W. Baks, P. Westbergh, J.S. Gustavsson and A. Larsson, “A 71 Gb/s NRZ modulated 850 nm VCSEL-based optical link”, IEEE Photon. Techn. Lett., accepted for publication (2014).
[29] D.M. Kuchta, A.V. Rylyakov, C.L. Schow, J.E. Proesel, C. Baks, P. Westbergh, J.S. Gustavsson and A. Larsson, “A 50 Gb/s NRZ modulated 850 nm VCSEL transmitter operating error-free to 90°C”, IEEE J. Lightwave Technol., accepted for publication (2014).
[30] N. Bamiedakis, J. Chen, P. Westbergh, J.S. Gustavsson, A. Larsson, R.V. Penty and I.H. White, “40 Gb/s data transmission over a 1 m long multimode polymer spiral waveguide for board level optical interconnects”, IEEE J. Lightwave Technol., accepted for publication (2014).
[31] G. Fiol, J.A. Lott, N.N. Ledentsov and D. Bimberg, “Multimode optical fiber transmission at 25 Gbit/s over 300 m with small spectral width 850 nm VCSELs”, Electron. Lett. 47, 810-811 (2011).
[32] R. Safaisini, K. Szczerba, P. Westbergh, E. Haglund, B. Kögel, J.S. Gustavsson, A. Larsson, M. Karlsson and P.A. Andrekson, “High speed 850 nm quasi-single mode VCSELs for extended reach optical interconnects”, IEEE J. Opt. Commun. Netw. 5, 686-695 (2013).
[33] Å. Haglund, J.S. Gustavsson, J. Vukusic, P. Modh and A. Larsson, “Single fundamental mode output power exceeding 6 mW from VCSELs with a shallow surface relief”, IEEE Photon. Techn. Lett. 16-18, 368-370 (2004).
[34] R. Safaisini, E. Haglund, P. Westbergh, J.S. Gustavsson and A. Larsson, ”20 Gbit/s data transmission over 2 km multimode fibre using 850 nm mode filter VCSEL”, Electron. Lett. 50, 40-42 (2014).
[35] P. Westbergh. J.S. Gustavsson and A. Larsson, “VCSEL arrays for multicore fiber interconnects with an aggregate capacity of 240 Gbit/s”, IEEE Photon. Techn. Lett., accepted for publication (2014).